fined similarly as Eq. (4)], in a He-Ne plasma with 8% helium-ion concentration. The two values of the plasma densities are plotted to show the density dependence of the resonance frequency. We observe ω_{res} approaches ω_{IH} as the density is increased which is in agreement with the theory. As shown by the figure, the measured damping increases rapidly as the wave approaches the resonance frequency. The curves are theoretical values calculated using the experimentally measured parameters. In the calculation, the ion-ion collisions among different ion species (which is the dominant process here) and the ion-neutral collisions are included. The effect of ion viscous damping,[12] $\gamma_i \propto \nu_{ii}(k_\perp \rho_i)^2$ is not included since in this experiment, the wave did not reach the $(k_\perp \rho_i)^2 \sim 1$ regime because of the heavy damping. Since the measured ion concentration has some uncertainties [here $(8 \pm 2)\%$ helium], the calculation was carried out for a range of concentration. From the plot in Fig. 3(b), we see that the best-fitted curve to experimental points is 8.5% helium which is well within the concentration uncertainty, and thus we conclude that the observed damping rate agrees well with theory.

In conclusion, the low-frequency resonance-cone behavior associated with the cold electrostatic ion-cyclotron wave was verified experimentally. With a slow-wave structure, the wave dispersion relation was measured which yielded a strong resonance behavior near the ion-ion hybrid resonance frequency. When $\omega/k_\parallel V_e < 3.0$, the wave was observed to damp heavily by electron Landau damping. As ω approaches ω_{res}, the wave damping was observed to increase rapidly due to the ion-ion collisions. Throughout the experiment, the measured values were found to agree well with theory.

The author would like to thank K. L. Wong for useful discussions and M. Porkolab and T. Stix for helpful comments. He also thanks J. Taylor, W. L. Hsu, R. Ernst, and R. Wilson for their technical assistance. This work was supported by the U. S. Department of Energy, Contract No. EY-76-C-02-3073.

[1]F. W. Perkins, Nucl. Fusion 17, 1197. This also gives references to earlier work.
[2]T. H. Stix, *Theory of Plasma Waves* (McGraw-Hill, New York, 1962).
[3]B. D. Fried and S. D. Conte, *The Plasma Dispersion Function* (Academic, New York, 1961).
[4]S. J. Buchsbaum, Phys. Fluids 3, 418 (1960).
[5]M. Ono, R. P. H. Chang, and M. Porkolab, Phys. Rev. Lett. 38, 962 (1977).
[6]M. Ono, Ph.D. thesis, Princeton University, 1978 (unpublished).
[7]P. K. Fisher and R. W. Gould, Phys. Fluids 14, 857 (1971).
[8]H. H. Kuehl, Phys. Fluids 17, 1636 (1974).
[9]R. J. Briggs and R. R. Parker, Phys. Rev. Lett. 29, 852 (1972).
[10]P. M. Bellan and M. Porkolab, Phys. Rev. Lett. 34, 124 (1975).
[11]P. M. Bellan and M. Porkolab, Phys. Fluids 17, 1592 (1974), and 19, 995 (1976).
[12]M. Porkolab, Phys. Fluids 11, 834 (1968).

Small-Scale Magnetic Fluctuations Inside the Macrotor Tokamak

S. J. Zweben, C. R. Menyuk, and R. J. Taylor
Center for Plasma Physics and Fusion Engineering, University of California, Los Angeles, California 90024
(Received 15 January 1979)

Magnetic pickup loops inserted into the Macrotor tokamak have shown a broad spectrum of oscillation in B_r and B_p up to $f \approx 100$ kHz. The high-frequency $\tilde{B}_r$ have short radial and poloidal correlation lengths $L < 5$ cm, in contrast with the usual Mirnov oscillations with $f \approx 7$ kHz and $L >> 5$ cm. The observed magnitude $\Sigma|\tilde{B}_r|/B_T > 10^{-5}$, where the summation extends over all $f > 30$ kHz, is in the range in which such radial magnetic perturbations may be contributing to anomalous electron energy transport.

The persistent anomaly of electron energy confinement in tokamaks has recently stimulated discussion of magnetic-fluctuation–induced transport.[1-4] In this Letter we describe what we believe are the first observations of small-scale radial magnetic fluctuations inside a tokamak plasma. Such fluctuations can in theory cause enhanced radial energy flow through a local restructuring or destruction of the magnetic flux surfaces.

Most magnetic measurements in tokamaks have been made with pickup coils located outside the plasma.[5] All tokamaks have low-frequency ($f \approx 10$ kHz) surface disturbances in B_p (Mirnov oscillations), with a helical structure $\exp[i(m\theta + n\varphi)]$, where usually $m \approx q(a) < 5$ and $n = 1$ in the steady state. These large-scale oscillations are observed in Macrotor, but here we concentrate on the higher-frequency components of $\tilde{B}_r$ and $\tilde{B}_p$ which are smaller in magnitude but which may have more influence on transport.

Measurements of the internal magnetic field of a tokamak have been limited either because material probes inserted into a discharge melt as a result of thermal or runaway bombardment, or because the probes tend to perturb the plasma. Probe measurements have been reported, however, in the small and relatively cold LT-3 and Minimak tokamaks, in which the current penetration phase,[6] the major disruption,[7] and the low-m kink/tearing modes[8] have been diagnosed. High-frequency magnetic fluctuations, similar to those reported in this Letter, have also been observed recently at the Caltech tokamak.[9]

Macrotor is a low-field ($B_T < 3$ kG), large (minor radius $a = 45$ cm), cold ($T_e \approx 100$ eV), and therefore a very low-power-density tokamak in which glass test tubes can be inserted typically 15 cm into the discharge without damage to the tubes or perceptible perturbation of the plasma. Under such conditions magnetic pickup loops located inside the tubes can easily measure small fluctuating fields within the plasma.

An important prerequisite for the use of this technique is a convincing proof that the probes themselves are not creating or significantly distorting the local magnetic field fluctuations. We have made various checks for the presence of such a probe effect, and have concluded that the observable fluctuations in Macrotor are not affected by our probes. The main points are as follows: (1) The insertion of the tubes does not affect the plasma current ($I \approx 50$ kA), voltage ($V < 2$ V), density ($\bar{n}_e \approx 10^{12}$–$10^{13}$ cm^{-3}), or the uv light emission in their vicinity; (2) the magnetic structure (spectrum and correlation length) is the same when observed with coils inside both 2-cm and 0.6-cm diameter tubes; (3) the presence of a second probe < 1 cm away from a given probe does not affect the signals from the first probe; and (4) a pair of coils inside a single tube gives the same magnetic structure as do two coils each in a separate tube (one tube vertical, one horizontal). We note that his benign response of the plasma to the probes has not been checked for frequencies above 100 kHz, and cannot be assumed for perturbations which may have a scale length smaller than the probe radius (approximately equal to the ion gyroradius in Macrotor).

In Fig. 1 we show the general behavior of $\dot{B}_r$ measured by a coil located 10 cm inside the limiting aperature of the torus near the equatorial plane. Superimposed on the usual low-frequency coherent oscillation ($f \sim 7$ kHz) is an apparently incoherent and broadband higher-frequency structure. These high-frequency oscillations persist throughout the steady state of this discharge and have been observed in all discharges examined in Macrotor.

For the discharge of Fig. 1, $T_e(0) \simeq 100$ eV, $n_e(0) \simeq 4 \times 10^{12}$ cm^{-3}, $IV \simeq (50$ kA$)(2$ V$) = 100$ kW; thus the bulk electron energy confinement time is $\tau_E \simeq 1$ msec [assuming $T_e \propto (1 - r^2/a^2)$ and $n_e \propto \sqrt{T_e}$]. This value is roughly consistant with tokamak empirical scaling, but is much smaller than the expected neoclassical confinement in this low-density regime, indicating the dominance of anomalous electron energy transport in this case.

In Fig. 2(a) we show a digitally derived spectrum analysis of the B_r fluctuations in the discharge of Fig. 1. This spectrum was computed from data taken over 15–20 msec, and has been slide averaged in frequency over 5 kHz in this case. Examination of many such spectra has

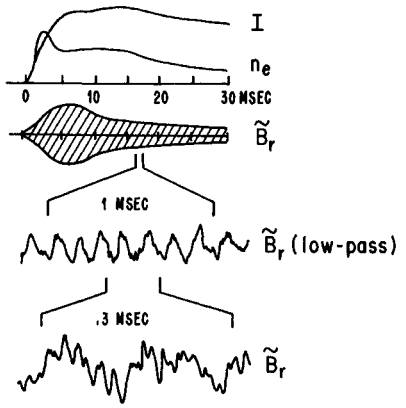

FIG. 1. Typical plasma current, density, and $\tilde{B}_r$ envelope are shown vs time ($I \simeq 50$ kA, $\bar{n}_e \simeq 2 \times 10^{12}$ cm^{-3} at 30 msec). The first expansion of $\tilde{B}_r$ is low-pass filtered to show clearly the Mirnov oscillations at $f \simeq 7$ kHz. The lower expansion shows the high-frequency structure without filtering.

shown that the high-frequency components ($f \gtrsim 30$ kHz) can be characterized by $|B_r| \propto f^{-n}$, where $n \simeq 1-2$, but that there is no reproducible or time-invariant mode structure in this spectral range. In contrast, the low-frequency oscillations often show a coherent structure such as that at $f \simeq 7$ kHz in this figure [this structure is most likely associated with the $m = 2$ tearing mode in these discharges with $q(a) \simeq 3$].

The variation of $|\tilde{B}_r|$ with probe position is shown in Fig. 2(b). The amplitude of the fluctuations increases strongly toward the center of the plasma, while the spectrum remains relatively unchanged (except for an attenuation of high-frequency components near the wall). The absolute magnitude of $\tilde{B}_r$ has been estimated using a bandpass filter to fix ω; we find, typically, that $|\tilde{B}_r| \simeq 10^{-2}$ G rms in the band 35–51 kHz full width at half maximum (FWHM) at 15 cm into the plasma, implying roughly that

$$\sum_{f>30\ \mathrm{kHz}} |\tilde{B}_r|/B_T \simeq 10^{-4}-10^{-5}$$

for the spectrum shown in Fig. 2(a). We have

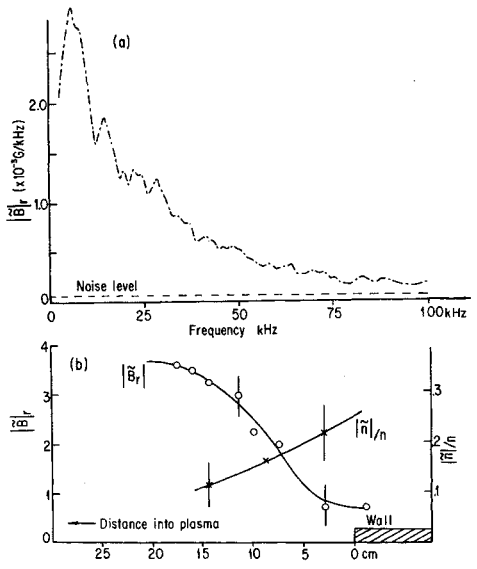

FIG. 2. (a) Spectrum of $\tilde{B}_r$ taken at 10 cm into the plasma during the steady state of a typical discharge. (b) The variation of $|\tilde{B}_r|$ vs coil position for $f \simeq 25$ kHz. The spectrum shape remains fairly constant over this range of coil positions. Also in (b) is $|\tilde{n}|_{\mathrm{rms}}/n$ profile as measured in the ion saturation current of a Langmuir probe. The ion-saturation-current profile itself looks similar to the profile of $|\tilde{B}_r|$.

also found generally that $\tilde{B}_p(\omega) \simeq \tilde{B}_r(\omega)$ in magnitude and spectrum, while $B_T(\omega) < 0.1 B_r(\omega) \simeq 0$. We note, incidentally, that the amplitude of the low-frequency mode has more variation during a particular discharge than does the amplitude of the higher-frequency structure, indicating that these two features are independent to a large extent.

Also shown in Fig. 2(b) is the profile of $|\tilde{n}|/n$ as measured by a Langmuir probe in ion saturation (the ion-saturation current profile itself looks like that shown for $|\tilde{B}_r|$). The spectrum of $n \approx (10^3-10^4)|\tilde{B}_r|/B_T$ for these discharges in which $\beta_T \approx 10^{-3}$ at 15 cm into the plasma. Note that the radial profile of $|\tilde{n}|$ is not similar to that of $|\tilde{B}_r|$.

In Fig. 3 we show an analysis of the cross correlation between two $\tilde{B}_r$ coils located inside a tube again inserted radially near the equatorial plane. In Fig. 3(a) is the spectrum of $\omega\tilde{B}_r$ measured at 10 cm into the plasma, while in 3(b) is the spectrum of $\omega\tilde{B}_r$ measured at 6 cm into the plasma in this case. In Fig. 3(c) is the cross correlation function, defined by

$$C(\tau) = T^{-1}\int_0^T S_1(t)\, S_2(t-\tau)\, dt, \qquad (1)$$

where S_1 and S_2 are the two probe signals, and the integral is over 4 msec of the steady-state discharge. In Fig. 3(d) is the correlation spectrum (frequency-resolved correlation coefficient)

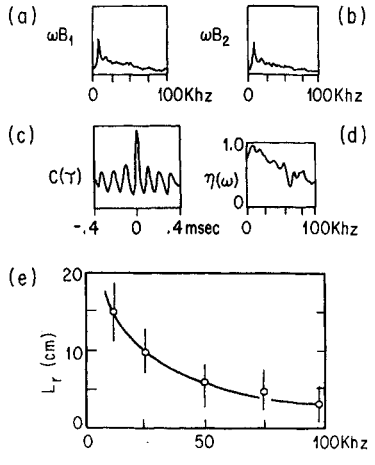

FIG. 3. (a), (b) Spectra of $\omega\tilde{B}_r$ for two coils radially separated by 4 cm, (c) cross-correlation function, and (d) correlation spectrum for this case. (e) Averaged radial correlation length vs frequency.

defined as[10]

$$\eta(\omega) \equiv \langle \eta(\omega) \rangle_{\Delta\omega} = |\langle F_1^*(\omega) F_2(\omega) \rangle| [\langle F_1^2(\omega) \rangle \langle F_2^2(\omega) \rangle]^{-1/2}, \quad (2)$$

where F_1 and F_2 are the Fourier transforms of S_1 and S_2, and where the angular brackets indicate averaging over $\Delta\omega \simeq 3$ kHz in the case of Fig. 3(d). This form of $\eta(\omega)$ is valid for our signals in which the peak of $C(\tau)$ at τ_p is such that $\tau_p \ll 1/\Delta\omega$.

Without averaging over $\Delta\omega$, $\eta(\omega) = 1$ (i.e., two pure sine waves are always correlated). With averaging over $\Delta\omega$, $\eta(\omega)$ for these signals converges to a value between 0 and 1 for $\Delta\omega \gtrsim 2$ kHz. Thus $\eta(\omega)$ measures the degree to which the two signals have a common structure within $\Delta\omega$, independent of phase. Note that, in practice, two completely uncorrelated signals (such as the drum noise of the two channels on which these signals are recorded) have $\eta(\omega) \simeq (0-20)\%$. Thus, a reasonable correlation exists when $\eta > 50\%$.

Inspection of these correlation spectra for various coil separations has shown a consistent pattern. For small radial separations (< 1 cm) the two signals are essentially identical and $\eta(\omega) \simeq 1$ for all frequencies. For a larger coil separation, the correlation is generally a decreasing function of frequency, as shown in Fig. 3(d), and the correlation at a particular frequency always decreases with increased coil separation. We take this to indicate that the average radial correlation length is decreasing with increased frequency. A quantitative evaluation of this effect is shown in Fig. 3(e), where we have defined a radial correlation length L_r as twice the coil separation at which $\eta(\omega) = 70\%$. This graph indicates that the high-frequency $\tilde{B}_r$ can have a small $L_r < 5$ cm, while at the same time the low-frequency Mirnov oscillations can have $5 \text{ cm} \ll L_r \lesssim a$, as expected for the low-m modes.

A similar analysis has been made for poloidal probe separations measureing $\tilde{B}_r$ or $\tilde{B}_p$ inside a tube inserted vertically 15 cm from the outer wall near the equatorial plane. The correlation lengths L_p are similar to those of L_r shown in Fig. 3(e). A measurement of the toroidal correlation length of $\tilde{B}_r$ with < 15 cm coil separation in the toroidal direction indicates that $L_T(\omega) \gg L_r(\omega)$.

Another basic property of these fluctuations is their phase velocity. As long as $\eta(\omega) > 50\%$, the phase difference $\Delta\varphi(\omega)$ between two coil signals is seen to be a smooth and reproducible function of frequency. We find that for a poloidal coil separation Δx, $\Delta\varphi \propto \omega \Delta x$ for all frequencies which satisfy the correlation condition (e.g., f < 60 kHz for $\Delta x = 2$ cm). The poloidal phase velocity is therefore roughly independent of frequency, and is estimated to be $\sim 10^6$ cm/sec in the electron diamagnetic drift direction. The calculated electron diamagnetic drift velocity is $(1-2) \times 10^5$ cm/sec, assuming the density scale length to be the minor radius.

We note that the autocorrelation time τ_A for these fluctuations can vary from $\tau_A \approx 1$ msec for cases in which there is a dominant low-frequency (coherent) component [e.g., Fig. 2(a)] to $\tau_A \approx 10$ μsec for cases in which the low-frequency component is relatively small. For the latter case, it seems clear that the phenomenon under consideration is broadband and turbulent in nature. If, however, one were to attempt a decomposition in terms of hypothesized short-lived (i.e., 10 μsec to 1 msec) coherent modes, one could estimate an $m \simeq 25$ corresponding to $f \simeq 100$ kHz (based on $m = 2$ at $f \simeq 7$ kHz, and a poloidal phase velocity independent of frequency). Yet the short poloidal correlation lengths (e.g., $L_p < 5$ cm at ~ 100 kHz) indicate that such modes can become decorrelated over only one poloidal wavelength, so that their structure is quite different from the globally correlated structure of the low-m modes.

The relevence of these fluctuations to anomalous transport can be studied through scaling experiments. We find $|\tilde{B}_r| \propto I$ at a fixed B_T, but the spectrum of $\tilde{B}_r$ does not change significantly between $q(a) \simeq 3-6$. We have also found that neither the amplitude nor the spectrum of $\tilde{B}_r$ changes significantly during gas puffing when $\bar{n}_e$ increases from 10^{12} cm^{-3} to $> 5 \times 10^{12}$ cm^{-3} with $\tau_E \propto n_e$. The most noticeable change with increased density is a decrease in the radial correlation length of $\tilde{B}_r$, perhaps indicating that the radial step size for transport decreases with increased density. However, a conclusive statement relating these fluctuations to anomalous losses cannot yet be made.

We thank J. D. Callen for discussions which helped lead to these experiments. This work was supported by the U. S. Department of Energy under Contract No. EY-76-C-03-0010. One of us (C.R.M.) is supported in part by the Fannie and John Hertz Foundation.

[1]J. D. Callen, Phys. Rev. Lett. 39, 1540 (1977).
[2]T. H. Stix, Nucl. Fusion 18, 353 (1978).

[3]A. B. Rechester and M. N. Rosenbluth, Phys. Rev. Lett. 40, 38 (1978).

[4]K. Molvig, J. E. Rice, and M. S. Tekula, Phys. Rev. Lett. 41, 1240 (1978).

[5]See, for instance, S. V. Mirnov and I. B. Semenov, in *Proceedings of the Sixth International Conference on Plasma Physics and Controlled Nuclear Fusion Research, Berchtesgaden, W. Germany, 1976* (International Atomic Energy Agency, Vienna, 1977), IAEA-CN-35/A9, p. 291; TFR Group, Nucl. Fusion 17, 1283 (1977); also, N. V. Ivanov, I. A. Kovan, and I. B. Semonov, Fiz. Plazmy 3, 960 (1977) [Sov. J. Plasma Phys. 3, 526 (1977)] for rf pickup measurements.

[6]J. D. Strachen, Nucl. Fusion 16, 433 (1976).

[7]I. H. Hutchinson, Phys. Rev. Lett. 37, 338 (1976).

[8]M. Makishima, T. Tominaga, H. Tohyama, and S. Yoshikawa, Phys. Rev. Lett. 36, 142 (1976).

[9]M. Hedemann and R. Gould, Bull. Am. Phys. Soc. 23, 873 (1978).

[10]See, for instance, G. M. Jenkins and D. G. Watts, *Spectral Analysis and Its Applications* (Holden-Day, San Francisco, 1968).

Dynamic Evolution of a *Z* Pinch

Dale Nielsen, James Green, and Oscar Buneman
Institute for Plasma Research, Stanford University, Stanford, California 94305
(Received 3 April 1978)

Three-dimensional, electromagnetic computer simulation experiments are presented showing the evolution of plasma columns subjected to external electric and magnetic fields. The results of two experiments are presented here. In the first, self-confinement is achieved; in the second, as instability arises which drives the plasma into a helical configuration.

In this Letter we report some numerical plasma simulation experiments which have shown the formation of a Z pinch with its subsequent instability and transition into a helical configuration. These observations were made with a particle code called SPLASH which is three-dimensional, relativistic, and fully electromagnetic. With this code we have conducted a study of Z-pinch plasma columns using a variety of initial velocity and spatial distributions in the presence of external electric and magnetic fields of various strengths. Two such simulations will be reported here. Our initial interest was guided by a desire to study self-confinement according to the Bennett relation, as well as plasma transport across B. Our observations agree qualitatively with recent theoretical predictions by Montgomery, Turner, and Vahala using magnetohydrodynamic theory,[1] in that we found large-scale helical and possibly force-free structures to develop as a result of a current threshold instability.

The first experiment to be described was performed by initializing the plasma with zero drift in a columnar shape of Gaussian radial density profile. A large external magnetic field ($\beta \approx 3\%$) is applied uniformly throughout the plasma column and the simulation region with the field lines parallel to the axis of the column. Additionally, a strong uniform external electric field is applied along the column which serves to accelerate the ions and electrons in opposite directions, thus establishing significant currents ($B_0/B_{\mathrm{self}} \approx 4.5$). The simulation is periodic in space so that a particle which moves out one side of the simulation domain is returned at the opposite side with its same velocity.

After an initial acceleration phase the external electric field was turned off. In both of the simulations to be described here, external fields are simply applied everywhere. They are not generated from charge-current distributions on the boundaries of the simulation region. Hence transients or penetration processes associated with sudden changes of the external fields are not simulated realistically. Some time after turning off the external electric field, we turned off the external magnetic field as well, allowing the particles to drift in their own self-consistent electric and magnetic fields. At this point comparisons were made between measured values of the self-consistent $B_\theta(r)$, and values calculated for a plasma column with open-ended transverse boundaries. The excellent agreement between these values gave assurance that the "image" columns introduced by the periodic nature of the simulation did not generate significant spurious fields. It should be added that simulations preformed on mirror-confined plasmas using the

ERRATA

SUPPRESSION OF METALLIC IMPURITIES BY ELECTRON INJECTION IN A TOKAMAK. R. J. Taylor and Lena Oren [Phys. Rev. Lett. 42, 446 (1979)].

On page 448, the last sentence of the first paragraph should read "No significant change is seen in the C I line..." (not Cr II line as printed).

IMPLICATIONS OF GENERAL COVARIANCE AND MAXIMUM FOUR-DIMENSIONAL YANG-MILLS GAUGE SYMMETRY. J. P. Hsu [Phys. Rev. Lett. 42, 934 (1979)].

In Eq. (4) the quantity L' should read $-\frac{1}{2}\partial_\mu h_\nu{}^A \times \partial^\mu h^{\nu B} g_{AB}$. Instead of using a simple "spin-mass correspondence" (i.e., spin $\rightarrow$ mass and $h_\mu{}^{jk} \rightarrow h_\mu{}^i$) to estimate the ratio of two different forces in (18), one should use $dE_{\rm int}/dr$ to estimate the strength of the gravitational spin-force $F_{\rm sp}$, where $E_{\rm int}$ is the classical static approximation of the interaction energy given by the Lagrangian (5). One finds that $|F_{\rm sp}|$ has the same order of magnitude as the Newtonian force. The author wishes to thank Dr. M. Horne, Dr. J. Denker, Dr. B. Yurke, Dr. D. A. Long, and his colleagues at Southeastern Massachusetts University for discussions on this matter and various possible experimental tests.

SMALL-SCALE MAGNETIC FLUCTUATIONS INSIDE THE MACROTOR TOKAMAK. S. J. Zweben, C. R. Menyuk, and R. J. Taylor [Phys. Rev. Lett. 42, 1270 (1979)].

On page 1272, the second sentence of paragraph 2, column 2, should read "The spectrum of $\tilde{n}$ is quite similar to the spectrum of $\tilde{B}_r$, but $|\tilde{n}|/n \approx (10^3-10^4)|\tilde{B}_r|/B_T$ for these discharges in which $\beta_r \approx 10^{-3}$ at 15 cm into the plasma."

Also, the following reference should have been included among the first four references of this Letter: D. D'Ippolito, J. Drake, and Y. C. Lee, Bull. Am. Phys. Soc. 23, 867 (1978).